Phase distribution near the focus in systems of different Fresnel numbers

Yajun Li*

Institute of Electro-Optical Engineering, National Chiao Tung University, 1001 Ta Hsueh Road, Hsinchu, Taiwan 300, China

Received January 31, 1985; accepted June 3, 1985

Three-dimensional phase distribution near the focal plane is demonstrated by cross-section profiles of cophasal surfaces. The phase distribution in the focal plane and the phase anomaly in the focus are discussed in greater detail. Numerical results obtained are arranged systematically with Fresnel numbers sampled between 0.5 and 100, a sampling that covers conventional and unconventional cases.

1. INTRODUCTION

Phase distribution near the focus when a converging, monochromatic, spherical wave is diffracted at a circular aperture on an opaque screen has been treated by many authors after Gouy's discovery in 1890 of the so-called phase anomaly near the focus.[1–4] The extensive literature related to this subject is cited in Ref. 3.

Attention is now paid to the same problem, because in a number of publications[5–12] authors have revealed that, in principle, many of the classical results are merely special instances that are covered by more-general laws. For instance, classical authors[3] predicted that the cophasal surfaces in the immediate neighborhood of the focus are nearly plane, while Gouy[1] argued that a spherical converging light wave passing through its focus undergoes a rapid phase change of π rad. In this paper, it is shown that the cophasal surfaces near the focus are approximately spherical, that the rapidity of the phase change along a selected geometrical ray through the focus is directly proportional to the Fresnel number of the diffracting aperture, and that therefore Gouy's predictions of phase anomaly near the focus may describe phenomena in focusing systems only when their Fresnel numbers are considerably larger than unity. Moreover, phase distribution in the focal plane needs to be discussed, because in the focal plane an additional parabolic phase factor has to be taken into account if some of the assumptions underlying the classical investigations are modified.[7]

The numerical results obtained in this paper are displayed systematically by curves and cross-section profiles with the Fresnel number sampled between 0.5 and 100.

2. EXPRESSIONS OF PHASE DISTRIBUTION IN THE FOCAL REGION

When a uniform converging spherical wave working at a circular frequency ω emerges from a circular aperture in an opaque screen, it is seen that it travels along the z axis toward the geometrical focus at $x = y = z = 0$ (Fig. 1). By using the scalar theory of diffraction, it can be predicted that the behavior of the diffracted field is determined by the following parameters: A, amplitude; a, aperture radius; λ, wavelength; and f, focal length. The last three parameters can be combined into the Fresnel number $N = a^2/\lambda f$ and the f number $F = f/2a$.

In the present investigation, attention is centered on the phase behavior of the diffraction field near the focus, which is, apart from a periodic factor $\exp(-i\omega t)$, given by[6,7,11,12]

$$\phi_N(u_N, v_N) = \frac{1}{1 - u_N/2\pi N}\left[4F^2 u_N + \frac{1}{4\pi N} v_N^2\right] - \alpha(u_N, v_N) - \frac{\pi}{2}, \quad (\mathrm{mod}\ 2\pi). \tag{2.1}$$

This is the central equation of this paper. In this equation

$$u_N = 2\pi N \frac{z/f}{1 + z/f}, \tag{2.2a}$$

$$v_N = 2\pi N \frac{r/a}{1 + z/f} \qquad [r = (x^2 + y^2)^{1/2}], \tag{2.2b}$$

and

$$\sin\alpha = \frac{S}{(C^2 + S^2)^{1/2}}, \qquad \cos\alpha = \frac{C}{(C^2 + S^2)^{1/2}}, \tag{2.3}$$

with

$$C - iS = 2\int_0^1 J_0(v_N\rho)\exp\left(-\frac{i}{2}u_N\rho^2\right)\rho\,d\rho. \tag{2.4}$$

The notation (mod 2π) in Eq. (2.1) means that ϕ_N is indeterminate according to the extension of an additive multiple of 2π.

The multivalued function ϕ_N has a branch point at each zero of the intensity.[3] At all points other than the points of zero intensity, ϕ_N is continuous with respect to (u_N, v_N). In the special case of ($u_N = 0$, $v_N = 0$), i.e., at the geometrical focus (which is not a branch point), we obtain from Eq. (2.1) that

$$\phi_N(0, 0) = -\frac{\pi}{2} \pm m\pi, \qquad (m = 0, 1, 2, \ldots). \tag{2.5a}$$

We can then define

$$\phi_N(0, 0) = -\frac{\pi}{2} \tag{2.5b}$$

as the principal value of $\phi_N(0, 0)$.

0740-3232/85/101677-10$02.00

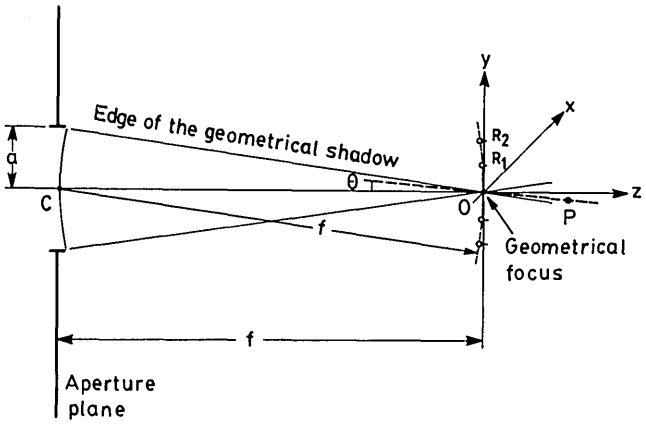

Fig. 1. Illustration of the notation.

3. PHASE DISTRIBUTION IN THE FOCAL PLANE

By putting $u_N = 0$ into Eq. (2.1), the following result is obtained:

$$\phi_N(0, v) = \frac{1}{4\pi N} v^2 - \alpha(0, v) - \frac{\pi}{2}, \quad (\text{mod } 2\pi). \quad (3.1)$$

In this equation the dimensionless parameter v_N, as defined by Eq. (2.2b), has been replaced by

$$v = 2\pi N \frac{r}{a}. \quad (3.2)$$

Under the condition $u_N = 0$, Eq. (2.4) yields the following results:

$$C = \text{Besinc}(v) = 2J_1(v)/v \quad \text{and} \quad S = 0. \quad (3.3)$$

By substituting these equations into Eqs. (2.3), we obtain

$$\sin\alpha = 0 \quad \text{and} \quad \cos\alpha = \text{Besinc}(v)/|\text{Besinc}(v)|. \quad (3.4)$$

From these results, it is clear that the principal value of $\alpha(0, v)$ in Eq. (3.1) is either 0 or π, according to whether the special function Besinc$(v) > 0$ or Besinc$(v) < 0$. These inequalities are equivalent, respectively, to

$$0 \le r < R_1, \quad R_{2p} < r < R_{2p+1}, \quad (3.5a)$$

and

$$R_{2p-1} < r < R_{2p}, \quad (p = 1, 2, 3, \ldots). \quad (3.5b)$$

Here R_p is the radius of the pth dark ring in the Airy pattern where the available regions of the following formulas are divided:

$$\phi_N(0, v) = \frac{1}{4\pi N} v^2 - \frac{\pi}{2} \quad (\text{mod } 2\pi) \quad (3.6a)$$

when inequalities (3.5a) hold, and

$$\phi_N(0, v) = \frac{1}{4\pi N} v^2 + \frac{\pi}{2} \quad (\text{mod } 2\pi) \quad (3.6b)$$

when inequalities (3.5b) hold.

Phase distributions in the focal plane are shown by the parabolic curves in Figs. 2(a), 2(b), 2(c), 2(d), 2(e), and 2(f) for systems of Fresnel number $N = 0.5, 1, 2, 5, 10, 100$, respectively. These parabolic curves are cut into segments by the points of zero intensity at $r = R_p$, at which the phase distribution undergoes rapid transitions of π rad. In addition, since calculations in the present study are limited to a region smaller than the fourth dark ring of the Airy pattern, the v values in

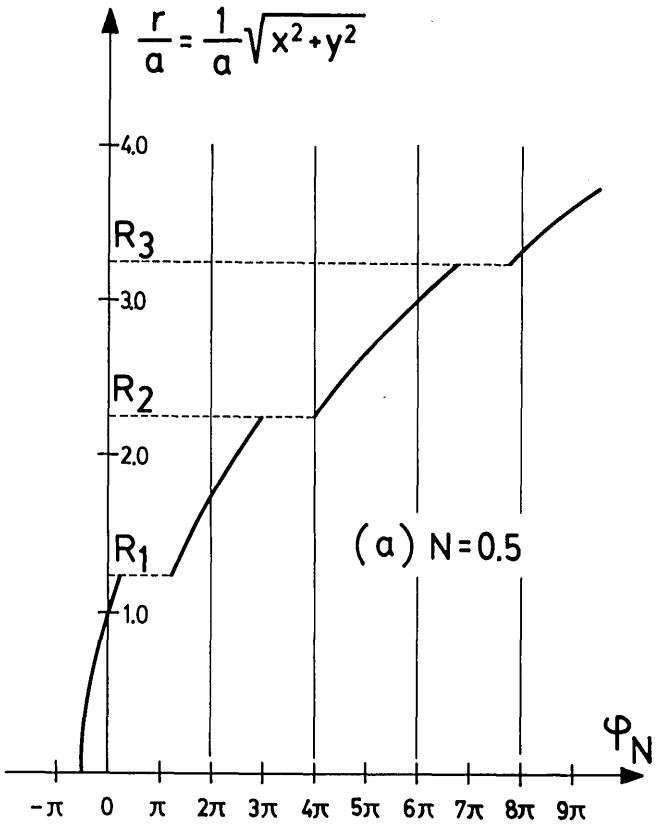

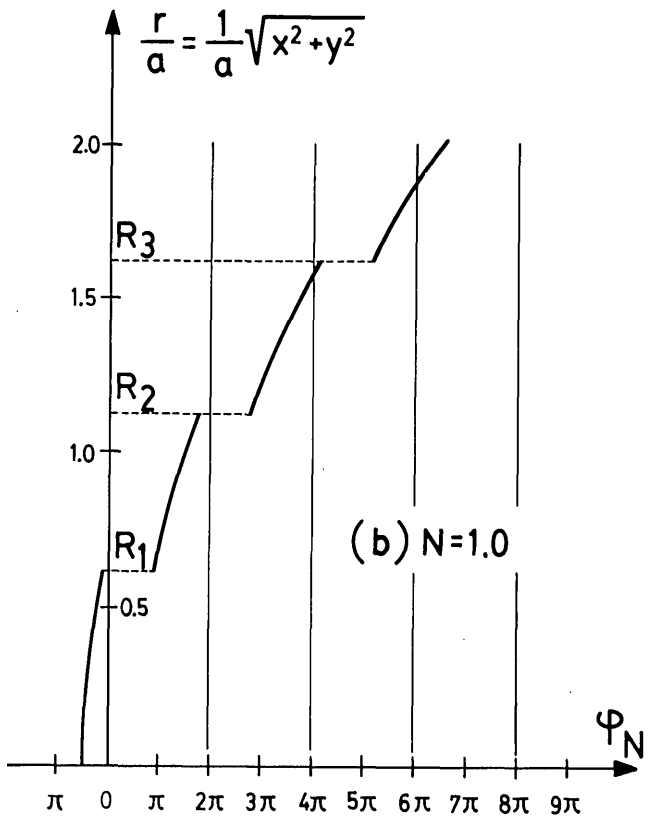

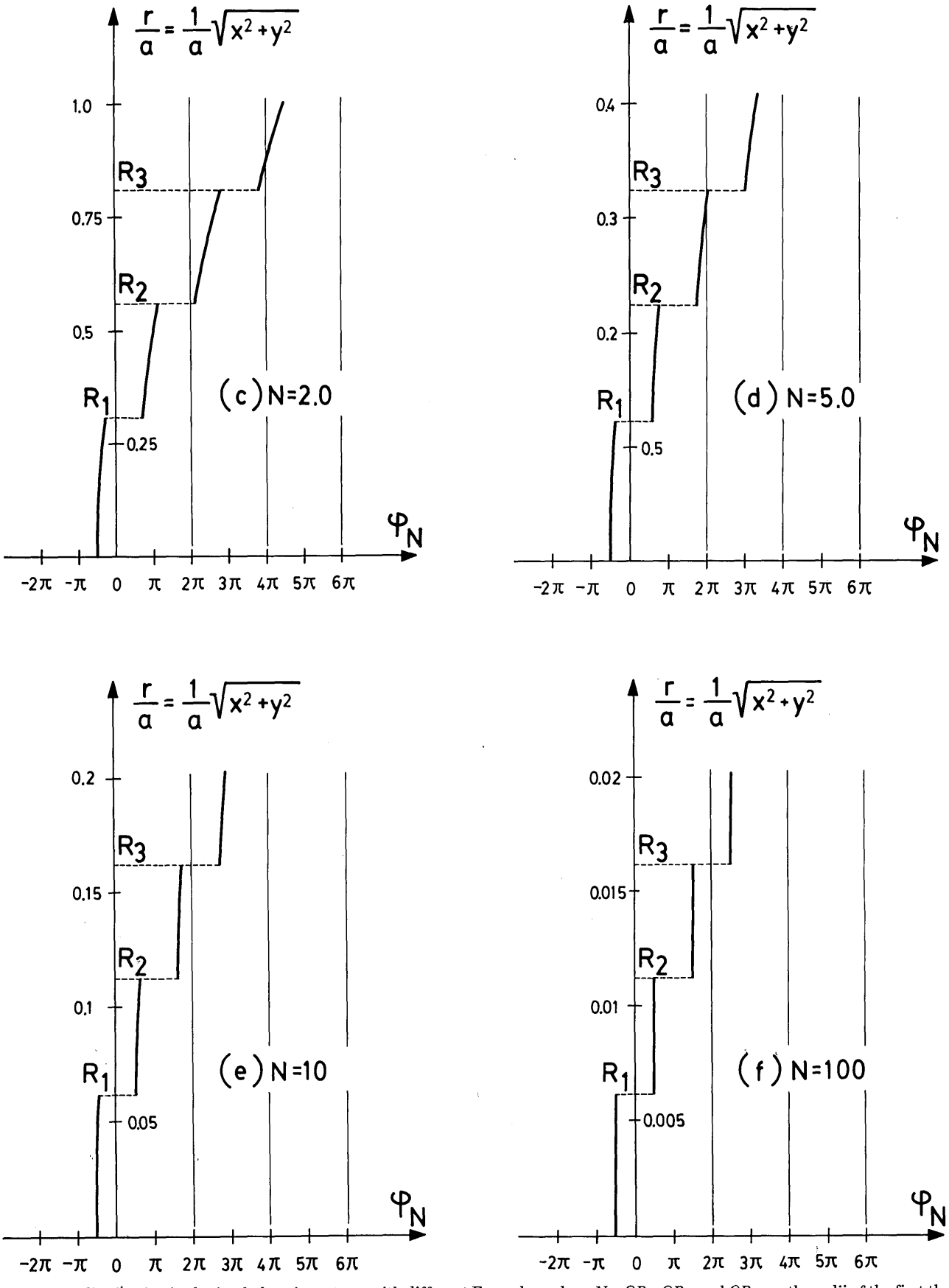

Fig. 2. Phase distribution in the focal plane in systems with different Fresnel numbers N. OR_1, OR_2, and OR_3 are the radii of the first three dark rings in the Airy pattern.

Eqs. (3.6) range from 0 to 13.32. A consequence of this limitation is that the contribution of the quadratic term on the right-hand sides of Eqs. (3.6) becomes negligible when the Fresnel number is much larger than unity. In Fig. 2(f) (N = 100), phase distribution between two adjacent dark rings of the Airy pattern is practically a constant—a result that may be regarded as classical and one that has not received much attention in the classical investigations.

Strictly speaking, a constant phase distribution in any finite area in the focal plane is unobtainable.

4. THREE-DIMENSIONAL PHASE DISTRIBUTION NEAR THE FOCAL PLANE

In order to illustrate the three-dimensional phase distribution near the focal plane by means of cophasal surfaces, Eq. (2.1) is treated as a transcendental equation, viz.,

$$\frac{1}{1-u_N/2\pi N}\left(4F^2u_N+\frac{1}{4\pi N}v_N{}^2\right)-\frac{1}{2}u_N+\beta(u_N,v_N)=\text{constant}, \tag{4.1}$$

in which $\beta(u_N, v_N)$ can be evaluated in terms of Lommel's U functions,[12] i.e.,

$$\sin\beta=\frac{U_2}{(U_1{}^2+U_2{}^2)^{1/2}},\qquad \cos\beta=\frac{U_1}{(U_1{}^2+U_2{}^2)^{1/2}}, \tag{4.2a}$$

or in terms of Lommel's V functions, i.e.,

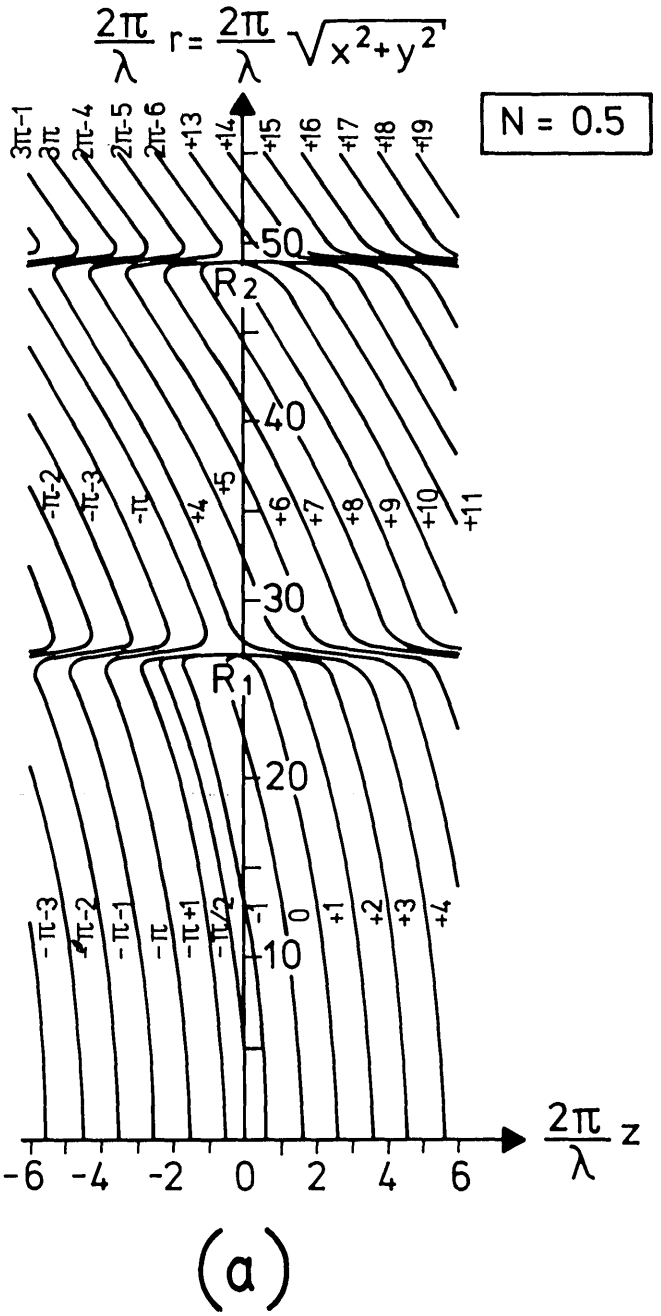

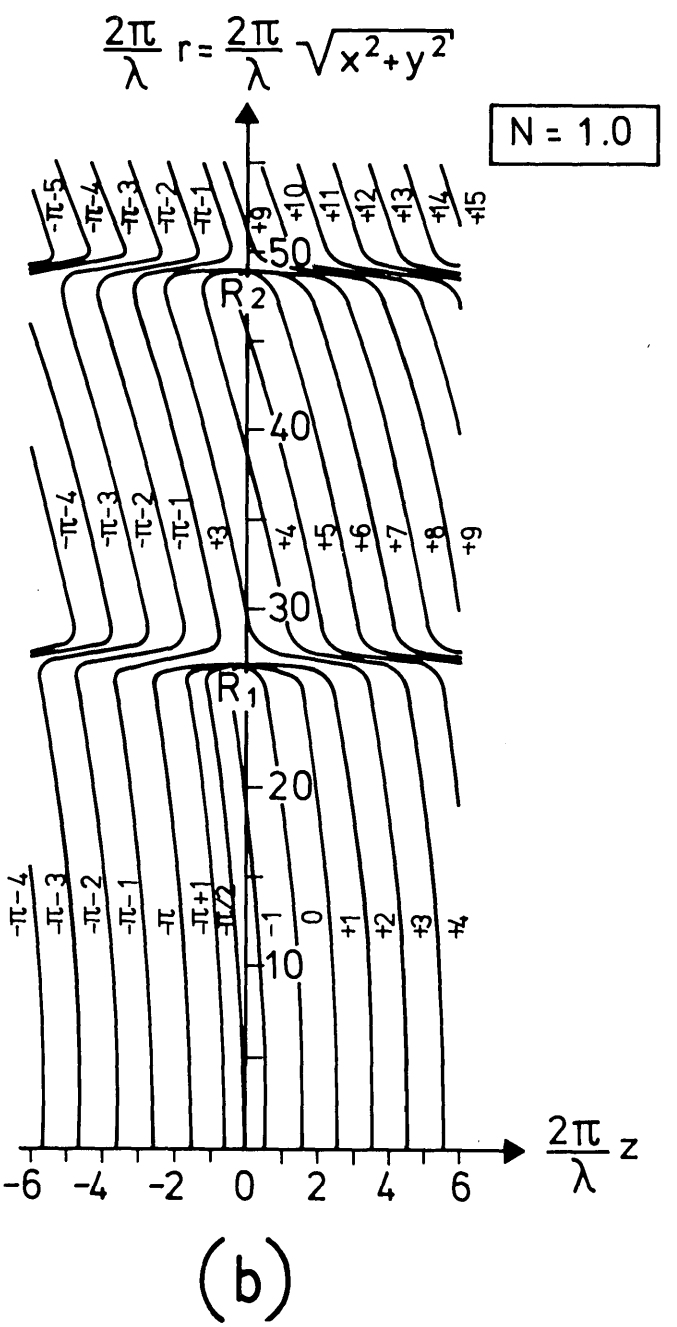

$$\sin\beta = \frac{V_0 - \cos\Theta}{[(V_0 - \cos\Theta)^2 + (V_1 + \sin\Theta)^2]^{1/2}},$$

$$\cos\beta = \frac{V_1 + \sin\Theta}{[(V_0 - \cos\Theta)^2 + (V_1 + \sin\Theta)^2]^{1/2}},$$

$$\Theta = \frac{1}{2}\left(u_N + \frac{v_N^2}{u_N}\right). \tag{4.2b}$$

The definitions of Lommel's U and V functions can be found in Ref. 13.

In this investigation, transcendental Eq. (4.1) was solved on a computer by employing Lommel's U functions when $|u_N/v_N| < 1$ and Lommel's V function when $|u_N/v_N| > 1$. The results obtained are displayed in Figs. 3(a)–3(f) by the profiles of cophasal surfaces in systems with different Fresnel numbers. In these figures, the curves are crowded in the region near the dark rings of the Airy pattern. In order to avoid overlapping, curves in those regions are displayed only schematically. Actually, phase structure near the said dark rings changed much more rapidly than is shown in Figs. 4(a)–4(f). From these figures, it seems clear that the cophasal surfaces near the focus are convex to the aperture and nearly spherical.

A further point of interest was a study of the curvature of cophasal surfaces at the focus. To undertake this, Eq. (2.1) was transformed into an implicit function with variables r and z, viz.,

$$G(z, r; \phi_N) = 0, \tag{4.3}$$

where ϕ_N = constant. From this, the said curvature is determined by

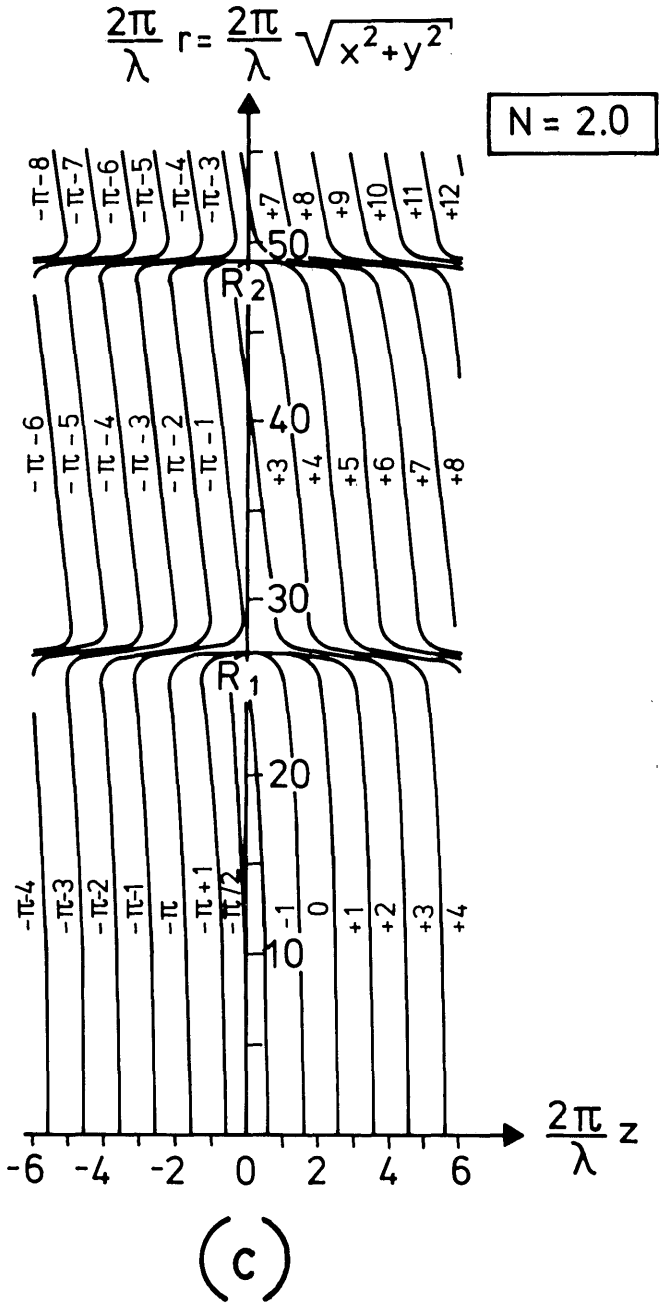

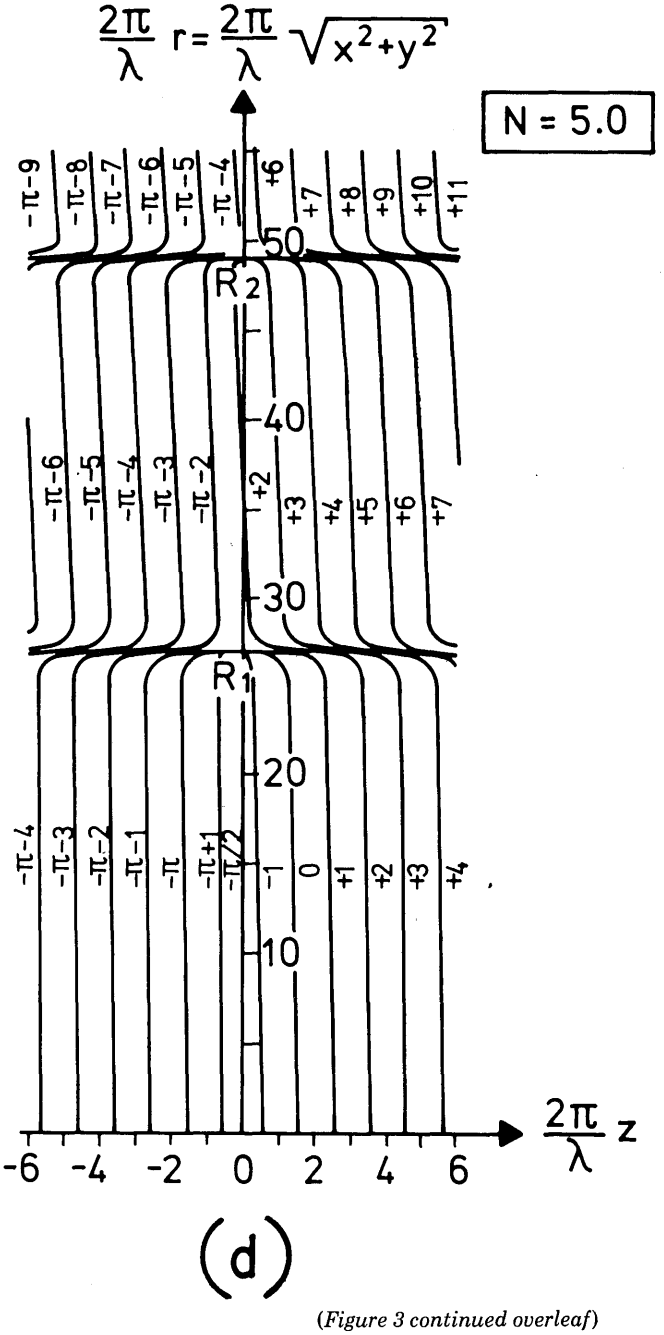

(Figure 3 continued overleaf)

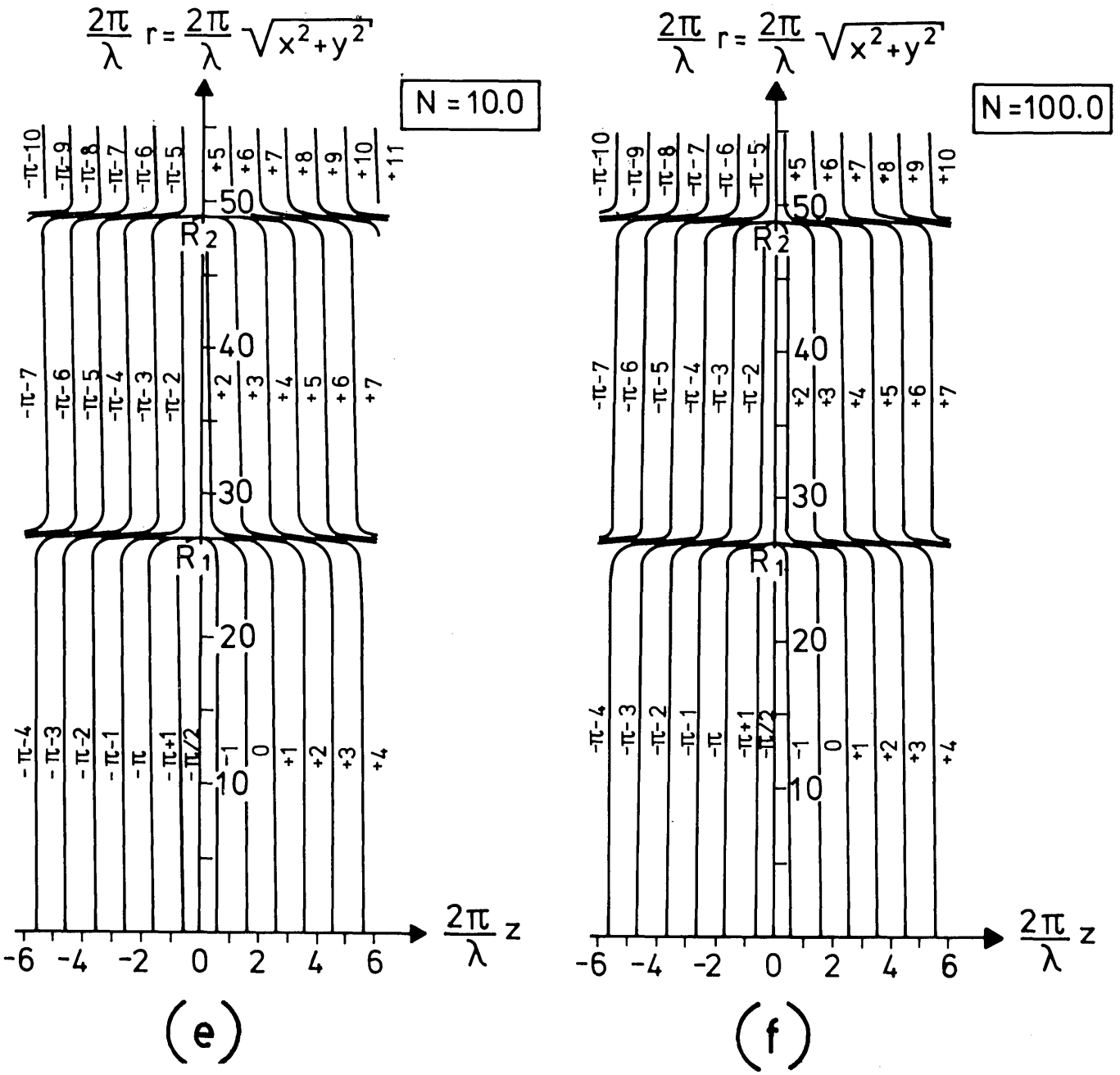

Fig. 3. Profiles of cophasal surfaces in the immediate neighborhood of the focal plane in an $F/3.5$ system with different Fresnel numbers N. OR_1 and OR_2 are radii of the first and the second dark rings in the Airy pattern.

$$\kappa = \left| \frac{G_z G_r (G_{zr} + G_{rz}) - (G_r)^2 G_{zz} - (G_z)^2 G_{rr}}{(G_z{}^2 + G_r{}^2)^{3/2}} \right|_{\substack{z=0 \\ r=0}}, \quad (4.4)$$

in which $G_z = \partial G/\partial z$, $G_r = \partial G/\partial r$, $G_{zr} = \partial^2 G/\partial z \partial r, \ldots$. After a lengthy derivation, omitted here, the result obtained can be expressed as

$$\kappa = \frac{1}{f(1 - 1/16F^2)}. \quad (4.5)$$

If $F^2 \gg 1$, the above relationship is reduced to $\kappa \simeq f^{-1}$; then the corresponding radius of curvature

$$\mathcal{R} = \frac{1}{\kappa} \simeq f \quad (4.6)$$

is obtained, a result that indicates that the center of the radius of curvature is in the middle of the aperture. This theoretical outcome, which may be regarded as a fundamental property for focusing systems of any Fresnel numbers, is shown graphically in Fig. 1 by the dashed circular curve. This outcome is also in close agreement with the experimental results obtained in microwave optics, as reported by Farnell (see Figs. 2 and 3 of Ref. 14).

The complete phase distribution near the focal plane can be found by rotating Fig. 3 around the z axis. After this has been done, the curvature circle in this figure becomes a sphere of radius f.

The classical prediction concerning the cophasal surfaces in the immediate neighborhood of the focus may be considered as a special case of the present result [expression (4.6)]. This is because the region in which the classical authors[3] carried out their calculations was limited by the first several dark rings in the Airy pattern, which, when the Fresnel number is far larger than unity, is rather small in comparison with a sphere of radius f. As a result of the limitation of the region of observation, it was logical for the classical authors to conclude that the cophasal surfaces in the immediate neighborhood of the focus are almost plane.

5. PHASE ANOMALY

In the classical theory of focusing, phase anomaly near the focus is an important subject that has attracted the attention of many investigators during the many years past. After numerous notable investigations, it is now generally accepted

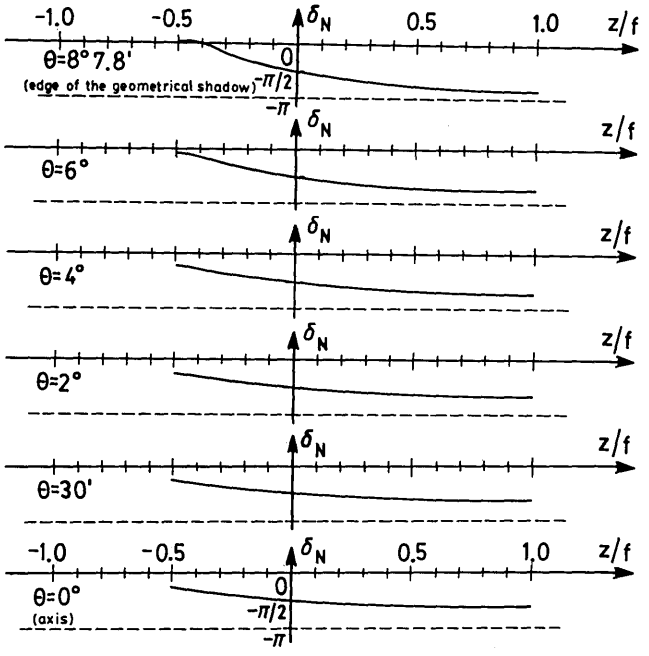

(a) N=0.5

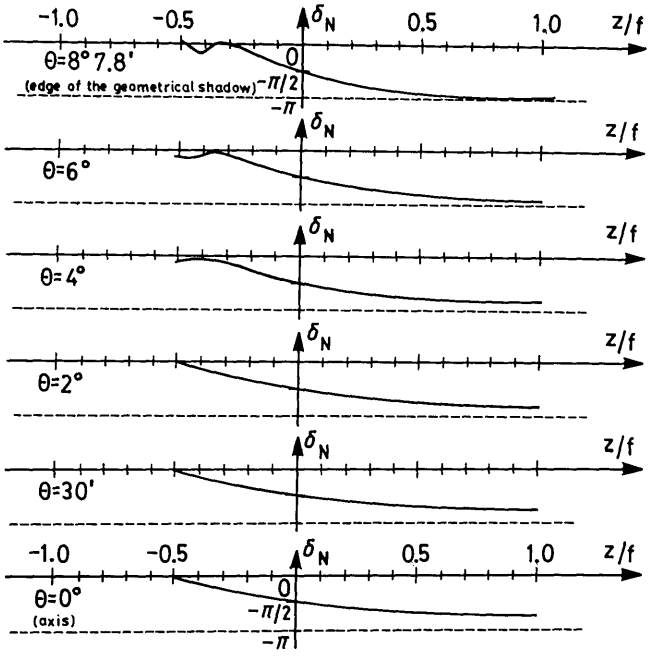

(b) N=1.0

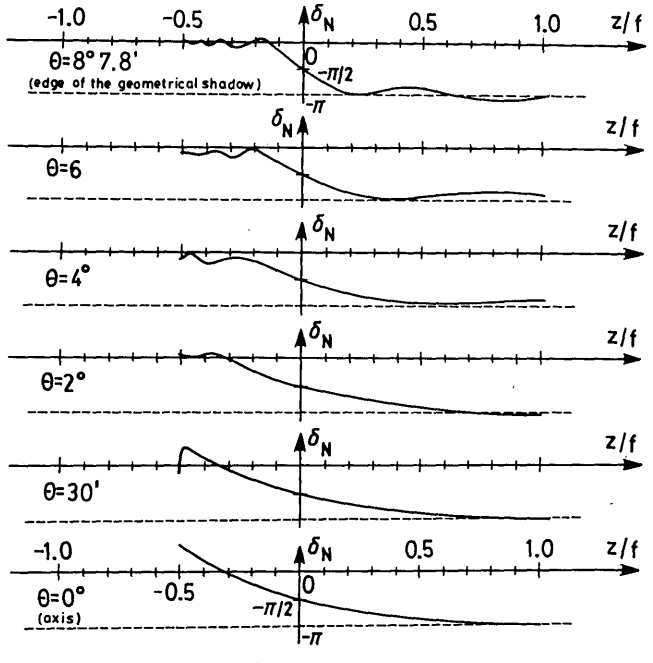

(c) N=2.0

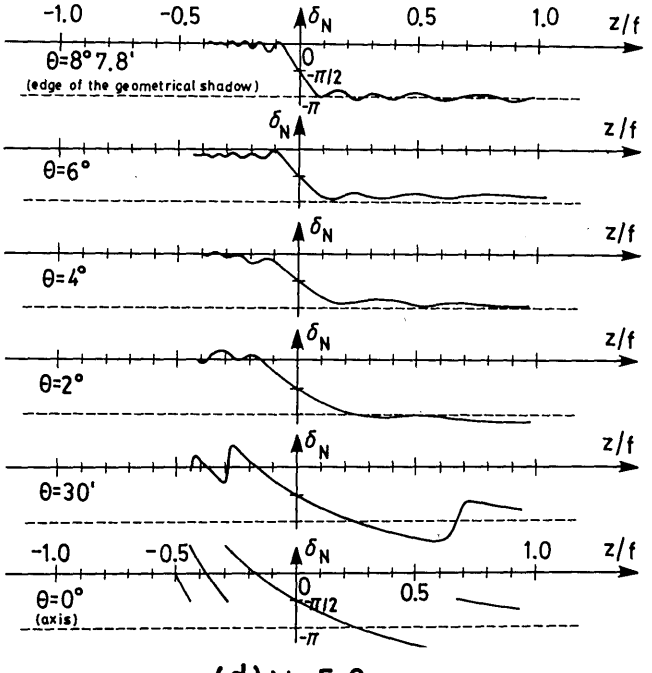

(d) N=5.0

(*Figure 4 continued overleaf*)

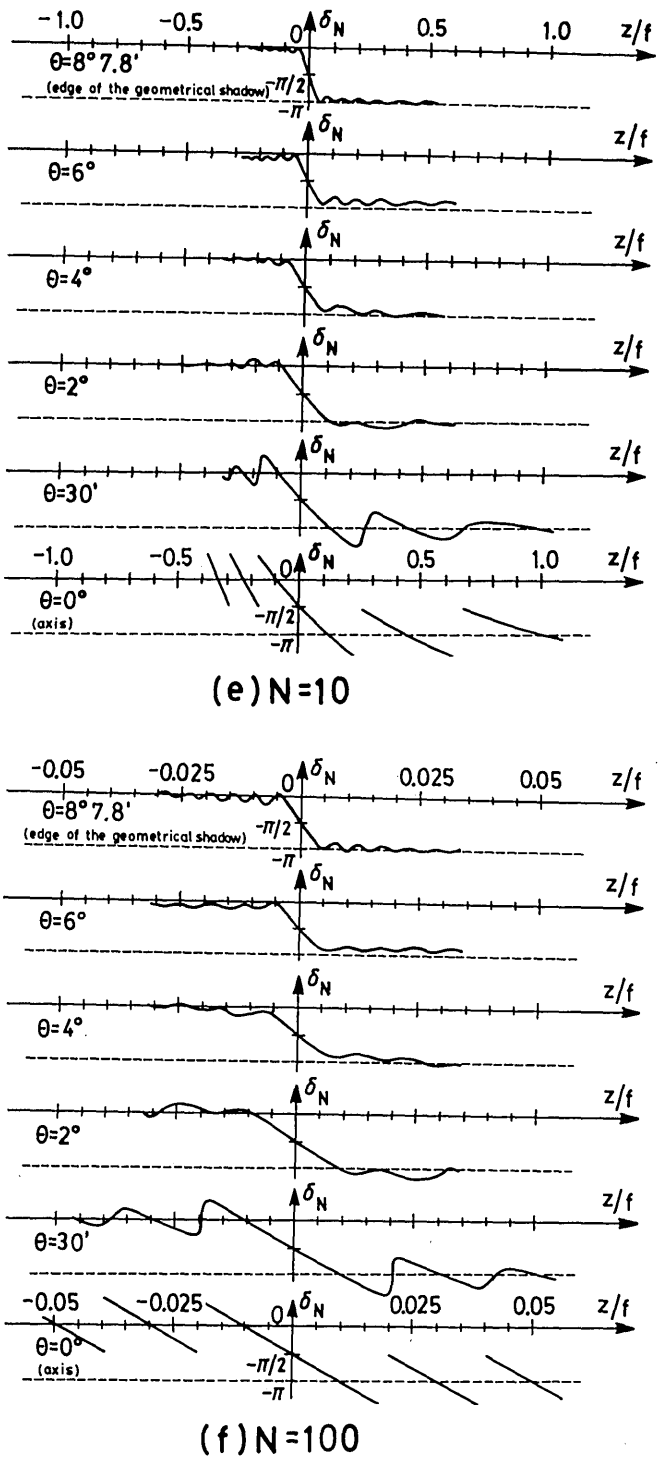

Fig. 4. Phase anomaly along geometrical rays through the focus in an $F/3.5$ system with different Fresnel numbers N. The angle θ denotes the inclination of the ray to the axis.

that a converging spherical wave undergoes a rapid phase change of π rad in passing through its focus.[1] This phenomenon is not only observable in focused light fields[2-4] but also in focused acoustic fields.

In this section of the present study, the classical predictions concerning phase anomaly near the focus are checked in systems of different Fresnel numbers. To this end, it is necessary to consider the phase behavior as the observation point P moves along a selected geometrical ray through the focus (see Fig. 1). If θ is the angle between the axis and the selected geometrical ray, then we have

$$\frac{v_N}{u_N} = 2F \tan\theta. \tag{5.1}$$

By inserting the above formula into Eq. (2.1), we obtain

$$\phi_N(u_N,\theta) = \frac{4F^2u_N}{1-u_N/2\pi N}\left(1+\frac{u_N}{4\pi N}\tan^2\theta\right) - \alpha(u_N,\theta) - \frac{\pi}{2} \pmod{2\pi}. \tag{5.2}$$

In order to determine the linearity in the phase change described by Eq. (5.2), we introduce a reference wave (geometrical wave). This wave has a linear phase property as observations are made in the region of illumination predicted by geometrical optics and along a ray through the focus, viz.,

$$D(P) = \frac{\exp[-i\tilde{\phi}(u_N,\theta)]}{R/f}, \qquad 0 \leqslant \theta \leqslant \tan^{-1}(2F), \tag{5.3}$$

where

$$\left.\begin{aligned}\tilde{\phi}(u_N,\theta) &= -kR \quad \text{when } u_N \leqslant 0\\ &= +kR \quad \text{when } u_N \geqslant 0\end{aligned}\right\}. \tag{5.4}$$

Here $k = 2\pi/\lambda$ is the wave number, and

$$R = (z^2+r^2)^{1/2} = \frac{1}{k}\frac{4F^2|u_N|}{1-u_N/2\pi N}\sec\theta \tag{5.5}$$

is the distance from point P to the focus 0. The difference

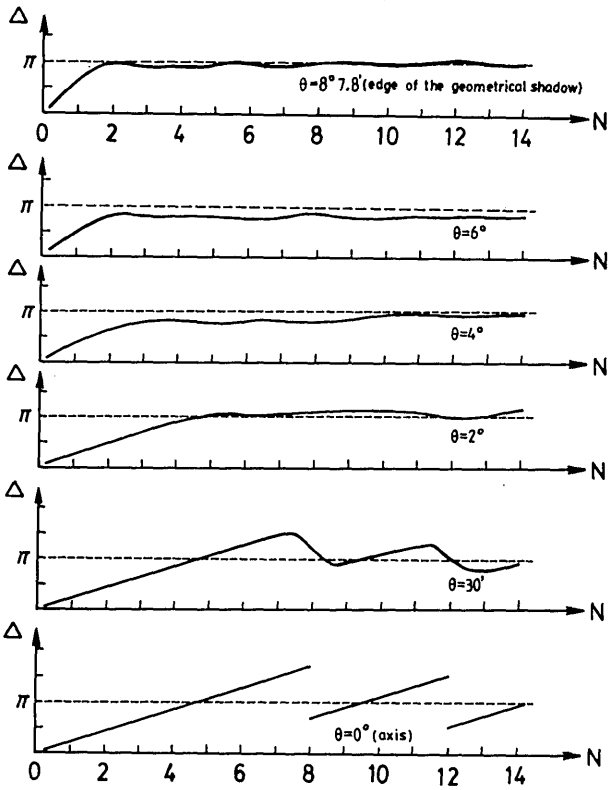

Fig. 5. Difference between phase anomaly δ_N evaluated at the points $z = -0.2f$ and $z = +0.2f$ in an $F/3.5$ system.

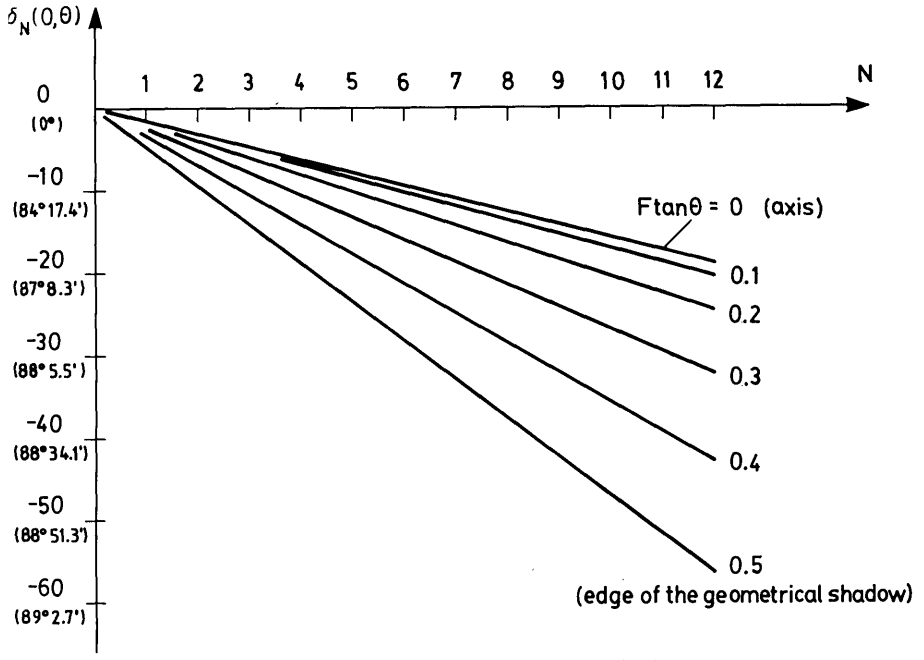

Fig. 6. Rapidity of the change of δ_N in the focus.

$$\delta_N(u_N, \theta) = \phi_N(u_N, \theta) - \tilde{\phi}(u_N, \theta), \tag{5.6}$$

$$= \frac{4F^2 u_N}{1 - u_N/2\pi N}\left[(1 - \sec\theta) + \frac{u_N}{4\pi N}\tan^2\theta\right] - \alpha(u_N, \theta) - \frac{\pi}{2}, \quad (\mathrm{mod}\ 2\pi),$$

$$0 \leqslant \tan\theta \leqslant (2F)^{-1}, \tag{5.7}$$

is called the phase anomaly along a geometrical ray. In order to compare this result with that given by the classical authors (see, e.g., Fig. 8.47 of Ref. 1), the same f number (i.e., $F/3.5$) is now adopted, and the influence of the Fresnel number on the phase anomaly is observed.

The results obtained from Eq. (5.7) are demonstrated in Fig. 4 for the same Fresnel numbers as those in Figs. 2 and 3. Each curve in Fig. 4 corresponds to a particular geometrical ray through the focus. Phase anomaly near the focus in a $N = 100$ focusing system [Fig. 4(f)] is essentially the same as the classical result, in which $\delta_N(u_N, 0)$ (phase anomaly along the axis) is a linear function of the z coordinate, except at the points of zero intensity; for the oblique rays, phase anomaly is antisymmetric to the focus and undergoes a rapid but continuous phase change of π rad as the rays pass through the focus. These properties, which are notable outcomes of the classical theory of the phase anomaly in the focus, disappear one by one with decreasing values of the Fresnel number N. Figures 4(e) ($N = 10$) and 4(d) ($N = 5$) show that phase anomaly is no longer antisymmetrical to the focus and that, along the axis and between two adjacent transitions, δ_N becomes a nonlinear function of the z coordinate. However, the change of δ_N near the focus is still π rad. But this property is lost when the Fresnel number is further decreased. Thus the classical theory can no longer be used to predict correct results when the Fresnel number is of the order of unity or smaller [see Figs. 4(a), 4(b), and 4(c) for the cases of $N = 0.5, 1, 2$].

Further evidence is provided by considering the following two quantities. First,

$$\Delta = \delta_N(u_N, \theta)_{z=-0.2f} - \delta_N(u_N, \theta)_{z=+0.2f}, \tag{5.8}$$

an index number expressing the total amount of the change of δ_N between two points on the two sides of the focus; and, second, a quantity concerning the rapidity of the change of δ_N in the focus,[15] viz.,

$$\delta_N'(0, \theta) = \left(\frac{\partial\delta_N}{\partial u_N}\frac{\mathrm{d}u_N}{\mathrm{d}z}\right)_{\substack{z=0 \\ u_N=0}} = \frac{\pi N}{2}[1 + 16F^2(\sec\theta - 1)], \quad 0 \leqslant \tan\theta \leqslant (2F)^{-1}. \tag{5.9}$$

This result indicates that the rapidity of the phase-anomaly change along a selected geometrical ray is directly proportional to the Fresnel number of the diffracting aperture.

Under the condition $F^2 \gg 1$, we have $\sec\theta - 1 \simeq 0.5\tan^2\theta$. We then obtain the following expression:

$$\delta_N'(0, \theta) = -\frac{\pi N}{2}[1 + 8(F\tan\theta)^2], \quad 0 \leqslant (F\tan\theta) \leqslant 0.5. \tag{5.10}$$

The quantity Δ is plotted in Fig. 5 as a function of the Fresnel number N. From this figure it is seen that the phase-anomaly change in the focal point and along the edge of the geometrical shadow attains π rad when $N \geq 2$, whereas phase anomaly along the axis attains the same amount of variation when $N \geq 5$. The rapidity of this variation [Eq. (5.10)] is demonstrated in Fig. 6, from which it is seen that an appreciably rapid phase change occurs in the focus only when $N > 10$. Therefore Gouy's prediction of the anomalous propagation of phase in the focus, i.e., a converging spherical wave undergoes a rapid π rad phase change in passing through its focus, may describe phenomenon in focusing systems only when their Fresnel numbers are considerably larger than unity.

6. CONCLUSIONS

In this paper, phase distribution near the focus is demonstrated by a series of diagrams. It seems that if these results are combined with the previous diagrams that show in detail the structure of the field and the distribution of encircled energy in the focal region,[11,12] a comprehensive knowledge of the focused field would then be obtained. For this purpose, the Fresnel numbers in Figs. 2–4 have been arranged in the same way as those used in the previous investigations.

ACKNOWLEDGMENT

I wish to thank E. Wolf for numerous helpful discussions concerning the subject matter of the present paper.

* Present address, Institute of Optical Sciences, National Central University, Chungli, Taiwan 320, China.

REFERENCES

1. M. Born and E. Wolf, *Principles of Optics*, 6th ed. (Pergamon, Oxford, 1980), Sec. 8.8.
2. A. Rubinowicz, "On the anomalous propagation of phase in the focus," Phys. Rev. **54**, 931–936 (1938).
3. E. H. Linfoot and E. Wolf, "Phase distribution near focus in an aberration-free diffraction image," Proc. Phys. Soc. London **69**, 823–832 (1956).
4. R. W. Boyd, "Intuitive explanation of the phase anomaly of focused light beams," J. Opt. Soc. Am. **70**, 877–880 (1980).
5. J. J. Stamnes, "Focusing of two-dimensional waves," J. Opt. Soc. Am. **71**, 15–31 (1981).
6. H. J. Erkkila and M. E. Rogers, "Diffracted field in the focal volume of a converging wave," J. Opt. Soc. Am. **71**, 904–905 (1981).
7. J. J. Stamnes and B. Spjelkavik, "Focusing of small angular aperture in the Debye and Kirchhoff approximations," Opt. Commun. **40**, 81–85 (1981).
8. E. Wolf and Y. Li, "Conditions for the validity of the Debye integral representation of focused fields," Opt. Commun. **39**, 205–210 (1981).
9. Y. Li and E. Wolf, "Focal shifts in diffracted converging spherical waves," Opt. Commun. **39**, 211–215 (1981).
10. Y. Li, "Dependence of the focal shift on Fresnel number and *f* number," J. Opt. Soc. Am. **72**, 770–774 (1982).
11. Y. Li, "Encircled energy for systems of different Fresnel numbers," Optik **64**, 207–218 (1983).
12. Y. Li and E. Wolf, "Three-dimensional intensity distribution near the focus in systems of different Fresnel numbers," J. Opt. Soc. Am. A **1**, 801–808 (1984).
13. G. W. Watson, *A Treatise on the Theory of Bessel Functions*, 2nd ed. (Cambridge U. Press, London, 1962), Sec. 16.5.
14. G. W. Farnell, "Measured phase distribution in the image space of a microwave lens," Can. J. Phys. **36**, 935–943 (1958).
15. Y. Li, "The anomalous propagation of phase in the focus: a reexamination," Opt. Commun. **53**, 359–363 (1985).